Experimental evaluation of interface adhesion of a flax fiber composite patch with epoxy and polyurethane adhesives for the reinforcement of steel structures

Mohamed Amine Tazi, Rosemere de Araujo Alves Lima, Enio Henrique Pires da Silva, Mouad Jebli, Sofia Teixeira de Freitas, Pascal Casari, Silvio de Barros

International Journal of Adhesion & Adhesives 129 (2024) 103559

Contents lists available at ScienceDirect

International Journal of Adhesion and Adhesives

journal homepage: www.elsevier.com/locate/ijadhadh

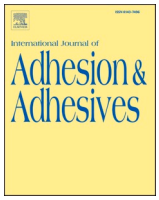

Experimental evaluation of interface adhesion of a flax fiber composite patch with epoxy and polyurethane adhesives for the reinforcement of steel structures

Mohamed Amine Tazi [a], Rosemere de Araujo Alves Lima [b], Enio Henrique Pires da Silva [c], Mouad Jebli [a], Sofia Teixeira De Freitas [b,d,*], Pascal Casari [e], Silvio de Barros [a]

[a] CESI LINEACT, France
[b] TU Delft, Netherlands
[c] University of São Paulo, Brazil
[d] IDMEC, Instituto Superior Técnico, Universidade de Lisboa, Lisboa, Portugal
[e] GeM Nantes University, France

ARTICLE INFO

Keywords:
Peel tests
Adhesion
Biobased adhesives
Flax fibers
Bi-material joints

ABSTRACT

Using fiber-reinforced composite patches for repairing damaged structures made of metal or/and concrete is an interesting and widely available solution on the market using synthetic materials. These repairing patches are bonded on the structures' surfaces to increase their strength against internal stresses, as well as protect them from external physico-chemical attacks, thereby limiting crack propagation. Natural fibers offer a potential alternative to replacing glass or carbon fibers commonly used for bonded repair patches. Similarly, bio-based polymers represent an important sustainable alternative for partially or entirely replacing the petroleum-based polymers. In this study, an epoxy matrix reinforced with flax fiber is proposed as the material for the patches, and bonded to a steel plate using four different types of adhesive materials, including a castor-oil derived polyurethane resin. Floating roller peel tests were performed to assess the adhesion and viability of these new patches. The resulting peeling loads and fracture surface analysis are presented. Polyurethane demonstrates promising performance for epoxy-to-steel joints, but major improvements of the bio-based polyurethane application process and curing conditions may be necessary for its successful industrial implementation.

1. Introduction

Composite materials are largely used in different industrial fields. Initially introduced in the aerospace sector [1, 2], the application of composites has been promptly expanded to many other fields such as automotive [3], maritime [4] and civil engineering [5, 6]. In most cases, infrastructures are subject to high loads, environmental aggressions, corrosion, and ageing, leading to rapid demand for the repair and reinforcement of damaged structures. The scientific community has recently been very active in exploring different repair techniques and finding solutions to prevent structural failure during their lifespan including composite patch systems [7].

Adhesive bonding technology is commonly the preferred method for joining composite structures, as it provides remarkable stress transfer mechanisms and design flexibility [8]. Moreover, unlike other joining methods, such as riveting and bolting, adhesive bonding induces less critical stress concentration areas by spreading the loads on wider surfaces, and does not adversely impact the mechanical substrates' properties. This manufacturing method depends on several parameters including the substrate type, surface treatment of bonded area and load specifications during service [9-12]. Composite repair technology seems to be the favored solution for the rehabilitation of many metallic structures such as pipes [4, 13], tanks [14] and ship hulls [15]. In the repair process, the Fiber-Reinforced Polymers (FRP) patch is usually applied using a wet lay-up process after adhesive application, thus regenerating the damaged structure's mechanical integrity, protecting it from internal stresses, and environmental aggressions [16].

So far, the majority of FRP materials used for structural purposes

* Corresponding author. TU Delft, Netherlands.
E-mail addresses: matazi@cesi.fr (M.A. Tazi), R.DeAraujoAlvesLima@tudelft.nl (R. de Araujo Alves Lima), eniopires@usp.br (E.H. Pires da Silva), mjebli@cesi.fr (M. Jebli), S.TeixeiraDeFreitas@tudelft.nl (S. Teixeira De Freitas), pascal.casari@univ-nantes.fr (P. Casari), sdebarros@cesi.fr (S. de Barros).

https://doi.org/10.1016/j.ijadhadh.2023.103559
Received 6 August 2023; Received in revised form 19 October 2023; Accepted 5 November 2023
Available online 8 November 2023

consist of either Carbon FRP (CFRP) or Glass FRP (GFRP) with epoxy resins manufactured from oil resources [9]. However, researchers have lately highlighted the non-degradability of synthetic composite materials, which is a major environmental concern. As a result, a huge interest in natural fiber composites with bio-resins has been expressed, as these materials are derived from renewable sources and address environmental issues [17, 18]. Plant-based natural fibers are widely available and offer ecological benefits. However, the main drawback of this kind of material is its lower mechanical strength compared to synthetic fibers, and its high moisture absorption, which harms the integrity of their properties.

In this study, an epoxy matrix reinforced with flax fibers (*Linum usitatissimum* L.) is proposed as a material for the patches. Flax is a typical plant-based resource, that exhibits varying properties based on many factors, such as climatic conditions during culturing, soil quality and water supply [19]. Compared to synthetic fibers like glass or carbon, flax is characterized by its low-density, cost-effectiveness and biodegradability. Moreover, it offers competitive mechanical properties [19-21]. *Baley et al.* [22], reviewed Flax fiber reinforced Polymers (FFRP), and examined the early works in the development of this type of FRPs and compared their mechanical properties with those of contemporary flax fibers. They claimed that flax fibers were first developed for aircraft parts in 1939, indicating that the potential for reinforcement of polymers by flax fibers was demonstrated over 80 years ago. Also, the mechanical properties of current flax composites are just slightly above those of the composites produced at that time. Nevertheless, our understanding of composite materials has significantly advanced over the years. Consequently, the focus should shift towards increasing the industrial implementation of FFRPs and fostering more competition among materials, representing the novelty in this field.

Regarding bonding quality, interface adhesion is one of the most critical parameters in ensuring the integrity of bonded joints. Kim et al. [23] reported that despite the well-established literature on metal-to-metal bonded joints and composite-to-composite bonded joints, the joining of dissimilar materials is relatively less explored. There exists a gap in the existing standardized testing procedures (ASTM and ISO) for evaluating the stiffness and strength of composite-to-metal adhesively bonded joints [24-27]. Additionally, while successful dissimilar material solutions have been developed for synthetic composite-metal combinations using glass and carbon fibers, there is limited research on Natural Fiber Composites (NFC) to metal adhesively bonded joints [28].

A particularly suitable test to analyze the interface adhesion properties of bonded joints (adhesive, co-bonded or co-cured) with dissimilar substrates under the most severe mode of loading (mode I), is the floating roller peel test. The floating roller peel test directs the evaluation to only one interface, unlike other peeling tests such as Double Cantilever Beam (DCB) or T-peel tests, where both interfaces are subjected to equal loads. Additionally, this type of peel test is easy, quick and reliable, making it applicable for various purposes, including adhesives screening tests, studying the effect of surface pre-treatment, and assessing bond durability [29, 30].

S. Teixeira de Freitas et al. [31, 32] successfully performed peel tests on composite-metal and composite-composite bonded joints. They emphasized that, during these tests, greater attention should be given to the failure mode rather than the failure load. Even in cases where cohesive failures occur, results showed that peel load values can be ten times lower when peeling off a composite adherend compared to a metallic one. In a different study, S. Teixeira de Freitas et al. [33] evaluated the effect of salt spray ageing on the adhesion characteristics of bonded composite-carbon steel joints using the roller peel test. They noticed that after 30 days of exposure, there was a minor reduction in both peel loads and failure modes, but after 90 days, there was a significant change. Peireira et al. [34] experimentally studied how adherends changes affect adhesion properties of brittle adhesives using the floating roller peel test, assessed the viability of using the floating roller peel test in composite-to-composite and composite-to-aluminum joints, and compared the performance of these joints with aluminum-aluminum joints. Their work also aimed to demonstrate how this test may be used to measure peel strength and conduct quality control on adhesion in joints made of composite materials.

Regarding polyurethane (PU), studies using this material as the adhesive in FRP-carbon steel structures and as the polymer matrix in FRP composite are rather uncommon in literature. In general, PU is less expensive than epoxy adhesives and shows a more ductile failure. Additionally, PU also shows higher flexibility, hardness, fatigue resistance and damage tolerance compared to epoxy resins [35]. The mechanical and thermal properties of two structural polyurethane adhesives used to bond Steel and CFRP were exanimated by Galvez et al. [36] in regard to humidity and temperature. This work by Galvez et al. made evident that moisture exposure and temperature control are essential for polyurethane adhesives to achieve their highest mechanical properties. Weiss et al. [37] focused on the ageing mechanisms of steel joints using polyurethane, coupling both the ageing of the polyurethane adhesive and the corrosion of the mild steel at high water activity.

These studies show promising results for using PU as the bonding adhesive for steel substrates. However, further investigations are required to fully understand the bond behavior between FFRP and steel with PU adhesives, especially knowing the wide range of chemical and structural variations that can be achieved with polyurethanes. These include but are not limited to temperature and load history effects, performance under hygro-thermal loading, creep behavior and effects of aggressive environment, to name few.

This paper aims to assess the interface adhesion properties between carbon steel and FFRP bonded joint through floating roller peel tests. Four different adhesives are used to bond the dissimilar substrates, including a castor-oil derived polyurethane resin as an alternative to synthetic adhesives. Peel loads, type of failure and quality of the adhesion for each type of adhesive are evaluated.

2. Materials

To evaluate the interface adhesion properties of a bonded joint between carbon steel and Flax Fiber Reinforced Polymer (FFRP), floating roller peel test specimens were manufactured. The specimens were prepared by bonding a carbon steel plate (flexible/parent adherend) with an FFRP plate (rigid substrate) using two bonding methods:

1 Co-curing: The flax fibers were impregnated with resin and co-cured directly onto a steel substrate. This method involved curing the FFRP simultaneously to bonding the steel substrate after the infusion process.
2 Secondary bonding: Firstly, a FFRP plate was cured, and secondly, bonded to the steel using three different adhesive materials. This method involved applying the adhesive between the cured FFRP plate and the steel substrate, and then allowing it to cure.

A carbon steel plate (S235/ASTM A36) with a modulus of elasticity of 200 GPa, a Poisson's ratio of 0.26 and a thickness of 1.76 ± 0.47 mm (average ± standard deviation) was selected as a parent substrate for the bonded joint. To prepare the composite material, a dry twill woven Flax fiber weighing 300 g/m^2 was used. The Flax fiber composite was manufactured using the bi-component epoxy SikaBiresin® CR83. Four adhesive materials were used to bond the substrates. Two bi-component epoxies from Sika®: Epoxy SikaBiresin® CR83 and Epoxy AxsonSika® ADEKIT A155/H9955. A single-component Polyurethane also from Sika®: Polyurethane Sikaflex®-554. And a bi-component Bio-Polyurethane derived from Castor Oil and developed by Kehl®, comprising a polyol and an isocyanate. The polyol has yellow colour and density of 1.0 g/cm^3. The isocyanate is composed by 4,4′- methylenediphenyl diisocyanate (MDI) with a density at 1.24 g/cm^3. Obtaining this BioPolyurethane involves reacting the diisocyanate with the

Table 1
Adhesive materials properties and type of bonding technique.

Specimens' nomenclature	Adhesive Material	Type	Tensile Strength [MPa]	Young's Modulus [GPa]	Bonding technique	Reference
Co-cured	Epoxy SikaBiresin® CR83	Bi-component	91	3.2	Co-curing	[38]
Epoxy	Epoxy AxsonSika® ADEKIT A155/ H9955	Bi-component	53	1.9	Secondary bonding	[39]
PU	Polyurethane Sikaflex®-554	Single-component	3.5	–	Secondary bonding	[40]
BioPU	Castor-oil-derived Polyurethane Kehl®	Bi-component	42	1.5	Secondary bonding	[41]

Table 2
Parameters for surface roughness analysis based on ISO 4287:1997 Standard.

Parameters	Lens magnification	λ_s filter	cut-off λ_c	evaluation length
Values	x500	$8\mu m$	$2.5mm$	$l_n = 5 \times \lambda_c = 12.5mm$

supplied castor-oil derived polyol at a ratio of 1:1 wt%.

Table 1 summarizes the adhesive materials used in the study, including their properties, and the associated bonding techniques employed to bond the dissimilar substrates.

3. Specimen manufacturing

3.1. Steel surface treatment

The carbon steel plate was sand-blasted and, then degreased using a cloth soaked with acetone to ensure a clean and oil-free surface. One additional cleaning step was done for the steel plates where PU and BioPU were used, which consisted of cleansing the surface with Sika® Aktivator-205 [42]. This extra-step was realized following the advice of a Sika operator, to achieve better adhesion.

The quality of the treated steel surface was analyzed using the Keyence® VHX-7000 Series numerical microscope. The surface roughness was measured according to the ISO 4287:1997 Standard [43]. Table 2

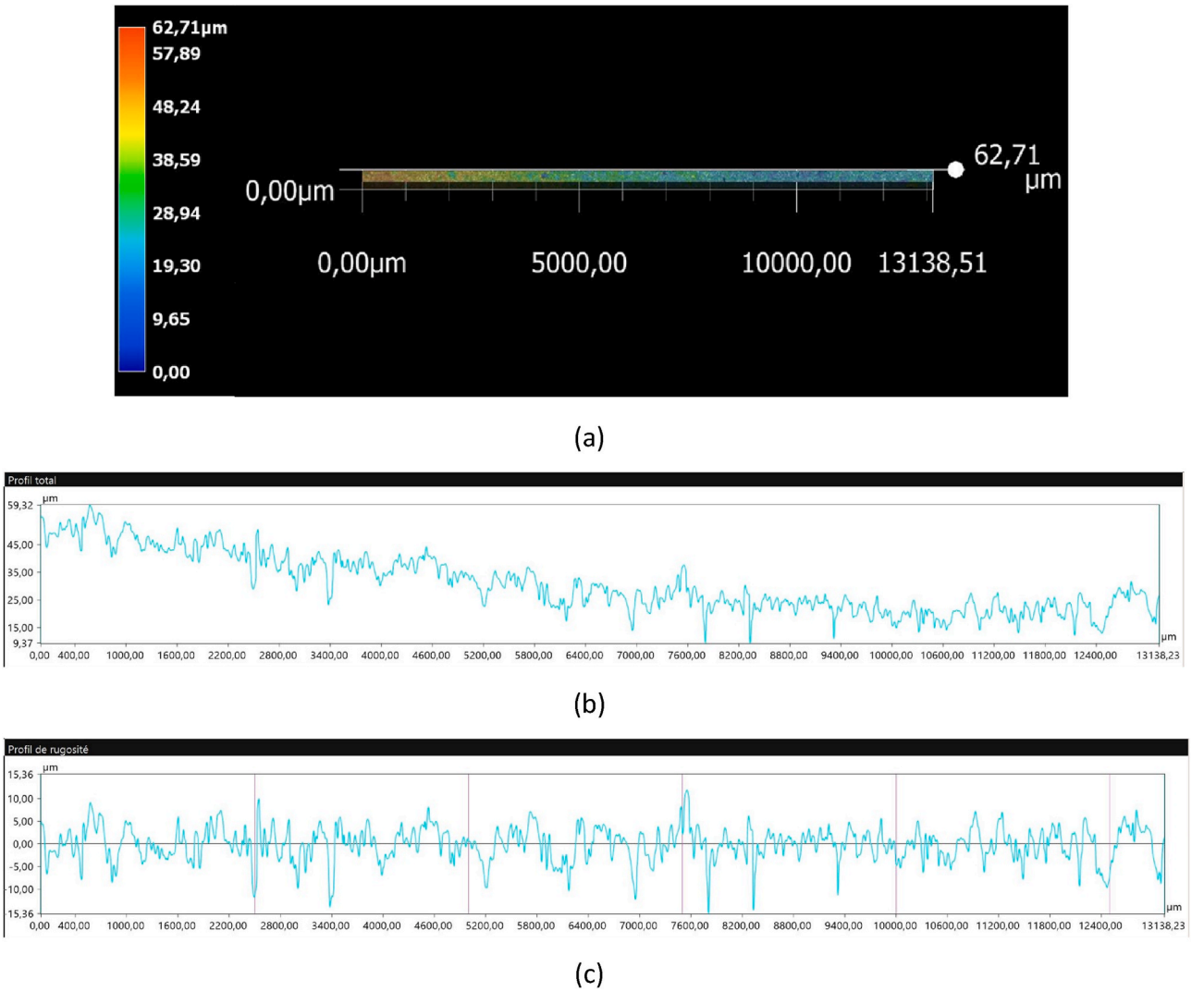

Fig. 1. Surface roughness analysis results, a) 3D representation, b) Total profile, c) Roughness profile.

Table 3
Average surface roughness parameters (Ra – Arithmetic Mean Deviation of the roughness profile, Rt – Total Height of roughness profile).

Ra (μm)	Rt (μm)
2.84	21.85

displays the specific microscope parameters used for the roughness analysis, and Fig. 1 presents the 3D surface profile of the sand-blasted steel plate. The obtained roughness parameters are presented in Table 3. To compare these obtained values, we cite Ghymatkar et al. [44] work where they studied the effect of different steel surface roughnesses on the adhesive bond strength. Different roughnesses were created using mechanical abrasion on a 3 mm thick mild steel (AISI 1045 medium carbon steel), and an optimum in average roughness was found at 1.97 µm. Sarlin et al. [24] also manufactured well bonded steel/-rubber joints by performing sand blasting on a 0.5 mm thick stainless steel sheet (AISI 304) and reached 2.46 µm average roughness.

3.2. FFRP plate manufacturing

The FFRP plates were manufactured using a vacuum infusion process. The epoxy resin SikaBiresin® CR83 was degassed under vacuum for 15 min prior to use. Twelve plies of Flax fiber, with a total mass of 275 g, were used for the laminate. The final layup configuration consisted of $[\pm 45^{\circ}]_{12}$ resulting in a plate thickness of 8.21 ± 0.41 mm (average ± standard deviation) and a total mass of 775 g. The curing process took place at room temperature and lasted for 24 h.

To prepare the surface of adhesion, the composite plate's surface was carefully sanded using sandpaper. Subsequently, any residual dust was removed using a clean cloth and by applying tape bands. These steps aimed to ensure proper adhesion and bonding between the FFRP plates and the steel substrates.

3.3. Adhesive application, substrate fixture and curing time

Four different materials were used to bond the dissimilar substrates following Table 1. The SikaBiresin® CR83 was used to co-cure the composite plate over the steel plate during infusion. Curing time was 24 h at room temperature. These specimens are hereby referred to as "co-cured".

For the three secondary bonded joints, adhesives were applied over the steel surface, the composite plate was placed on top, and pressure was imposed on the assembly using clamps and weights. The thickness of the joint was controlled using metallic wires with a diameter of 1 mm in the four extremities of the assembly – see Fig. 2. The curing time for all assemblies was 48 h at room temperature, under weight. A Polyethylene non-adherent film was introduced into the assemblies to create a 25 mm of crack initiation zone as shown in Fig. 3.

3.4. Water jet cutting of the specimens

Once cured, the bonded joints were cut with a water jet cutting machine TCIcutting® BP-C Series 1515. A cannon with a diameter of 0.72 mm was utilized for the cutting process. The cutting process was carried out under a water pressure of 3000 bar, using an Indian garnet 80 mesh abrasive agent with a 225 g/min flow rate. The cutting speed was set at 98 mm/min.

The final specimens' dimensions were in accordance with the standard test method ASTM D3167 [45] for floating roller peel tests for metal bonding. Specimens were 23.32 ± 0.54 mm (average ± standard deviation) wide, 300 mm long for the steel arm, 250 mm long for the

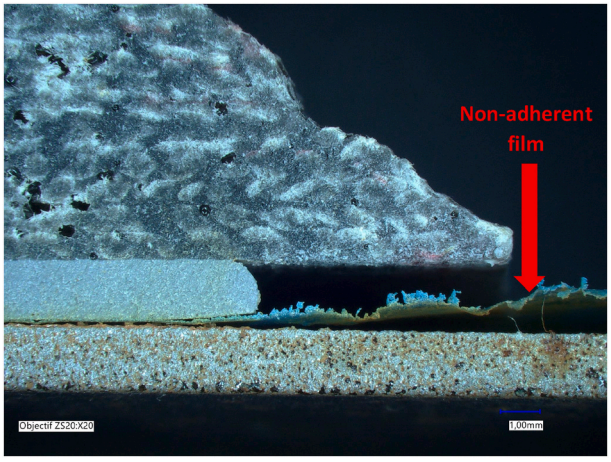

Fig. 3. Microscope image of the zone of crack initiation.

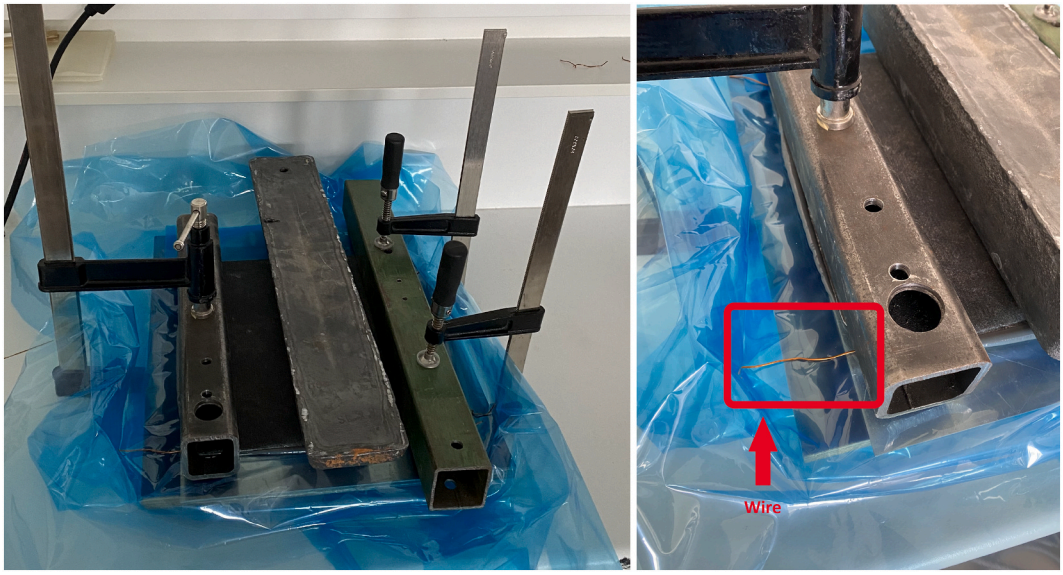

Fig. 2. Assembly set-up and adhesive thickness control.

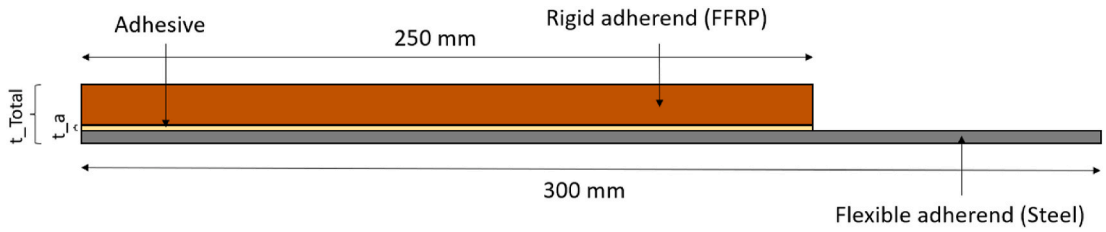

Fig. 4. Scheme of peel sample dimensions.
t_Total: Total thickness of specimens, and t_a: Adhesive thickness.

Table 4
Total specimen thickness and adhesive thickness.

Specimen type	Total thickness [mm]	Adhesive thickness [mm]
Co cured	9.59 ± 0.12	0
Epoxy	11.05 ± 0.37	1.32 ± 0.18
PU	11.26 ± 0.55	1.42 ± 0.39
BioPU	11.69 ± 1.34	1.22 ± 1.15

composite substrate. Fig. 4 shows the dimensions of the floating roller peel test specimens.

Table 4 lists the total specimens' thickness and adhesive thickness (average ± standard deviation) for each specimen type.

4. Experimental methods

The experimental testing involves conducting Standard Floating Roller Peel Tests (FRPT) on the four batches of specimens, - see Table 1. Three specimens were tested from each batch. During testing, the flexible adherend (Carbon Steel) is peeled off from the rigid adherend (FFRP).

The testing was carried out using an electro mechanic Zwick machine with a maximum capacity of 20 kN. The testing speed was set to 125 mm/min in accordance with the ASTM D3167 Standard [45]. To capture the crack propagation during the tests, a digital camera was used, recording at a frequency of 0.5 frames per second. Fig. 5 illustrates the set-up of the peel test.

During testing, load-displacement curves were recorded to assess the bonded joints' mechanical behavior.

5. Results and discussion

The results of peel tests, including the average peel load values and failure mechanisms observed for each type of specimens, are presented in Table 5. The average peel load values are shown as the average ± standard deviation of the three specimens tested for each adhesive type. Two distinct failure mechanism were observed: cohesive failure (CF) occurring within the adhesive layer, and adhesive failure (AF) at the interface between adhesive and adherends.

The percentage area of each failure modes was measured based on the visual observations of the specimens' fracture surfaces, using the Fiji

Table 5
Average peel loads and failure mechanisms.

Specimen type	Average peel load [N]	CF (%)	AF (%)
Co cured	–	30	70
Epoxy	272.6 ± 104.2	0	100
PU	807.7 ± 66.8	100	0
BioPU	74.8 ± 18.5	14	86

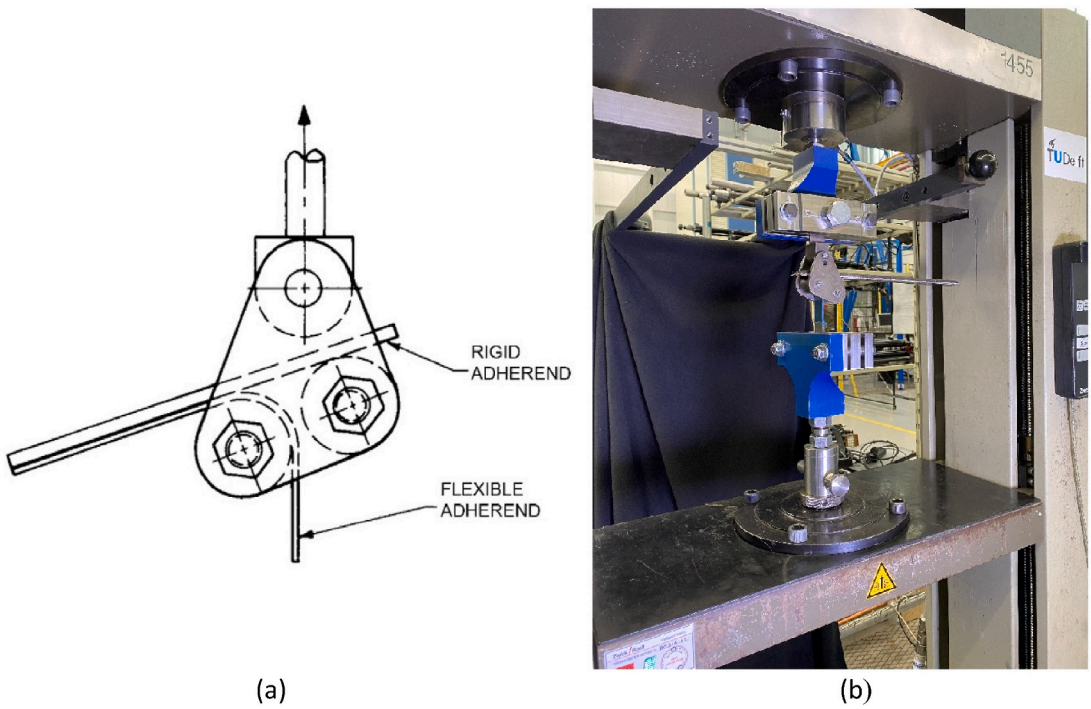

Fig. 5. a) Scheme of Floating roller peel test [33], b) Experimental set-up for floating roller peel tests.

Fig. 6. Example of cohesive failure areas (highlighted) for BioPU Specimen 1.

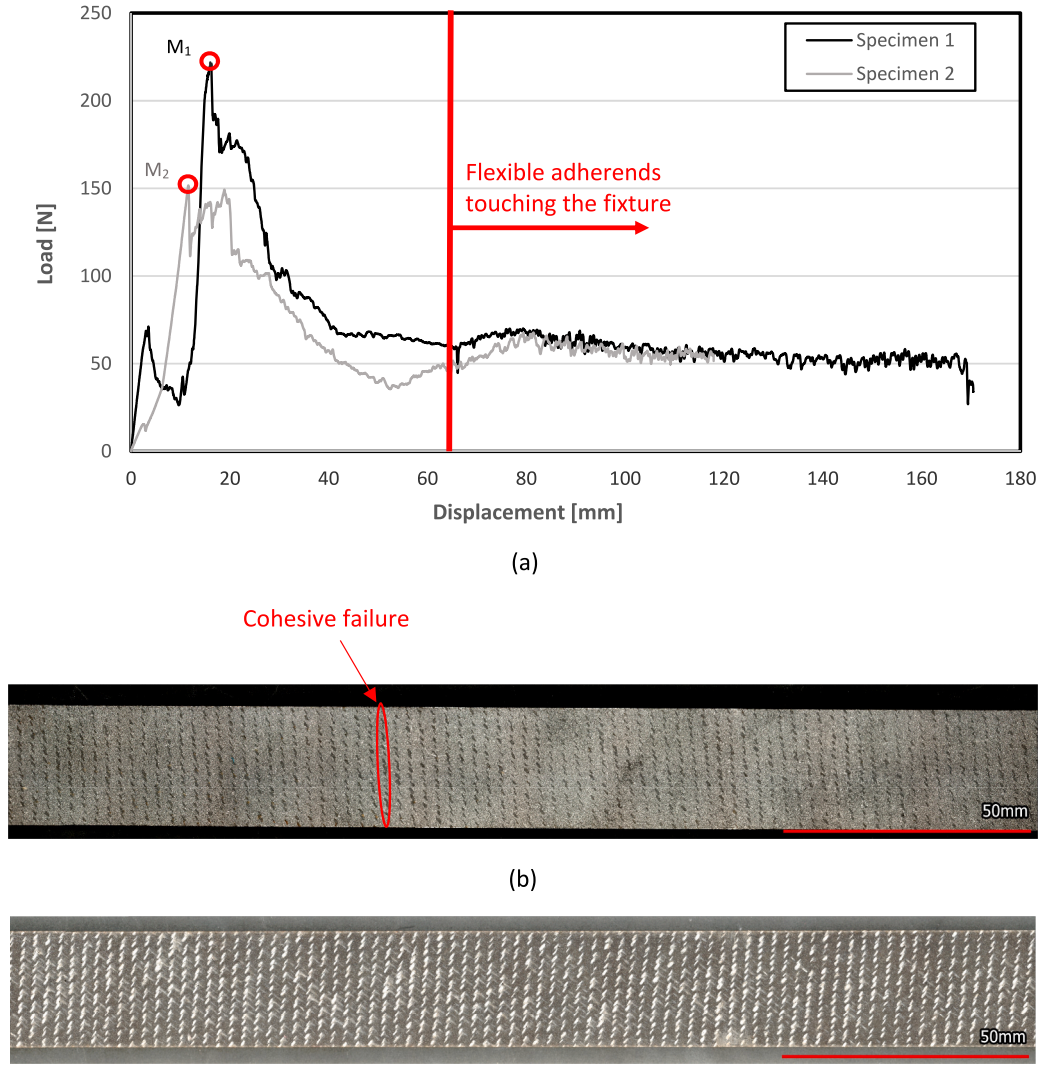

Fig. 7. a) Load-displacement curves for co-cured specimens (Epoxy SikaBiresin® CR83), and corresponding fracture surfaces for specimen 1, b) Steel interface and c) FFRP interface.

image processing package for scientific image analysis. Fig. 6 gives a representation of the realized measurements on one of the tested specimens.

The average failure peel load was determined over a displacement of 100 mm, excluding the first 50 mm. This procedure for calculating average failure peel load values aligns with ASTM standard D3167 [45] for peel tests.

The detailed results for each type of specimens are shown in the following subsections.

5.1. Co-cured

Fig. 7 shows the load-displacement curves recorded for two of the three co-cured samples (Epoxy SikaBiresin® CR83), and a representative fracture surfaces for specimen 1. It is worth mentioning that only two of these types of specimens are shown since the third test was considered invalid.

Different maximum load values for specimens 1 and 2 were observed - M_1 (222 N at 16 mm) and M_2 (151 N at 11.6 mm). After the maximum load, the load value decreased to a plateau value of approximately 60 N.

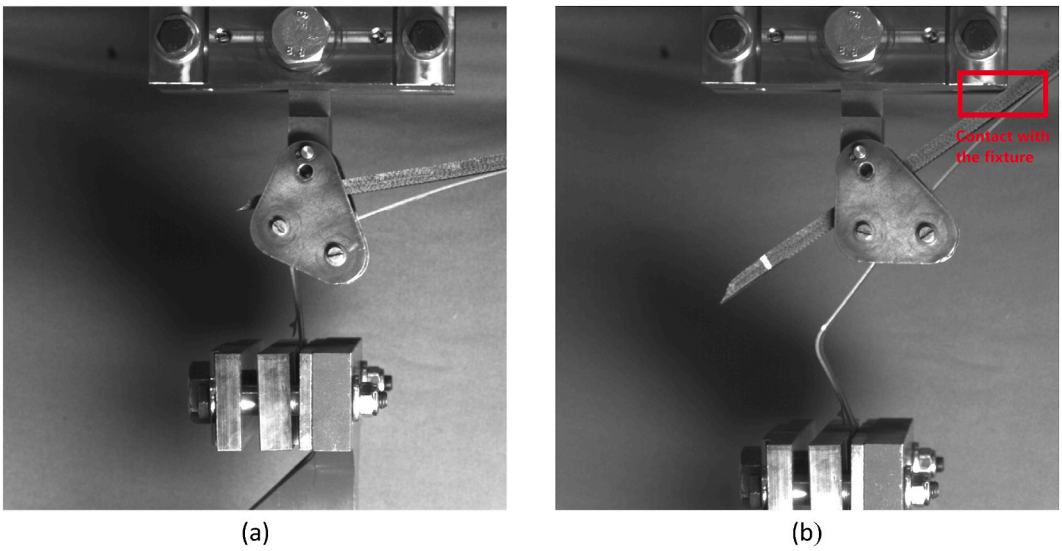

Fig. 8. Specimen 1 pictures, a) Debonding of the joint prior to bending of the steel on the roller – Image captured at 21 mm of displacement, b) Specimen making contact with machine fixture – Image captured at 67 mm of displacement.

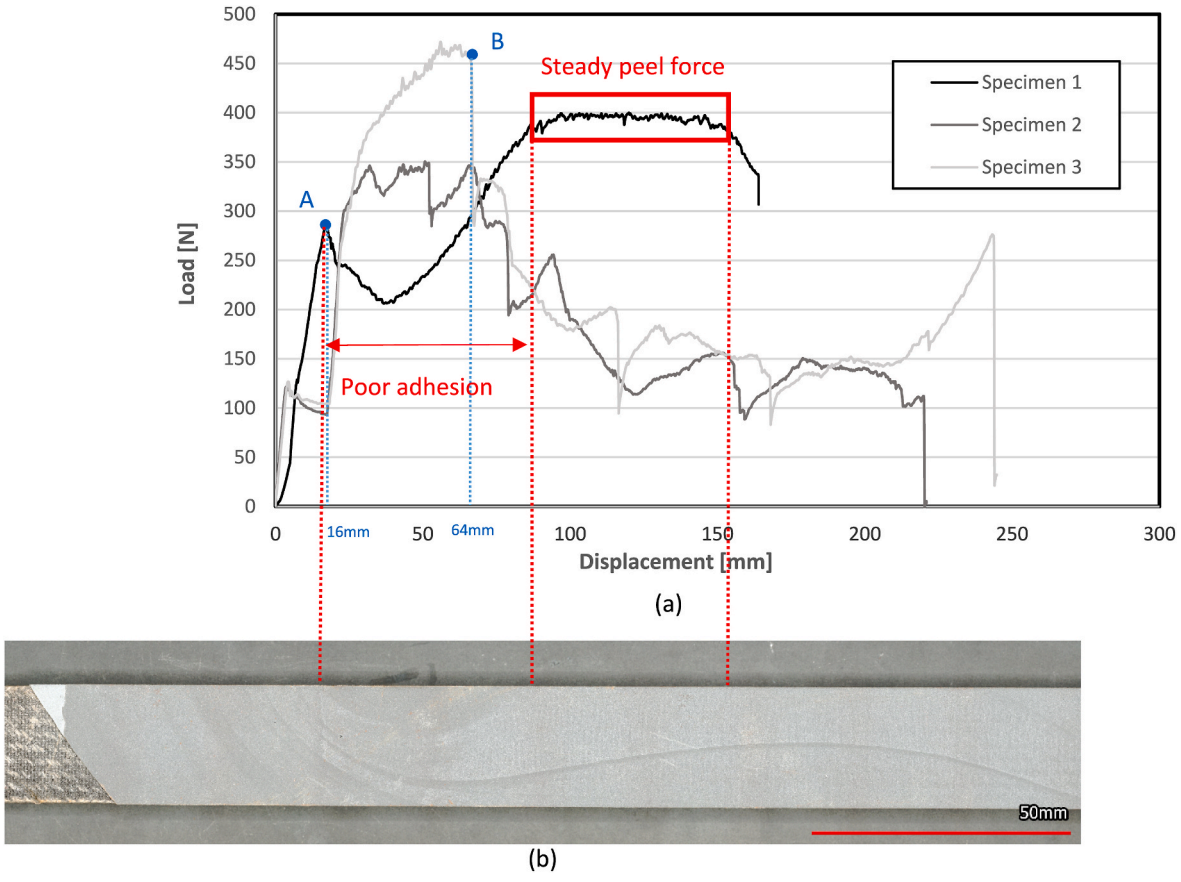

Fig. 9. a) Load-displacement curves for Epoxy Specimens (AxsonSika® ADEKIT A155/H9955), and b) corresponding fracture surface of composite rigid adherend for specimen 1.

After 65 mm displacement, the specimen touched the metallic upper part of the Zwick testing machine, resulting in unreliable peel load values.

The fracture surface reveals a mix between cohesive failure and adhesive failure, with the former being limited to the regions in contact with the fiber. The adhesive failure within the steel interface is predominant (70 %), which is not surprising knowing that co-cured specimens using epoxy resins are very demanding on substrate surface preparation. Visual observation reveals that insufficient resin flowed to the interface between the fibers and the steel during the infusion process.

The significant decrease in the load-displacement curve after the maximum peak, is therefore explained by poor adhesion at the interface, resulting in low peel force, and leading to debonding of the substrate to

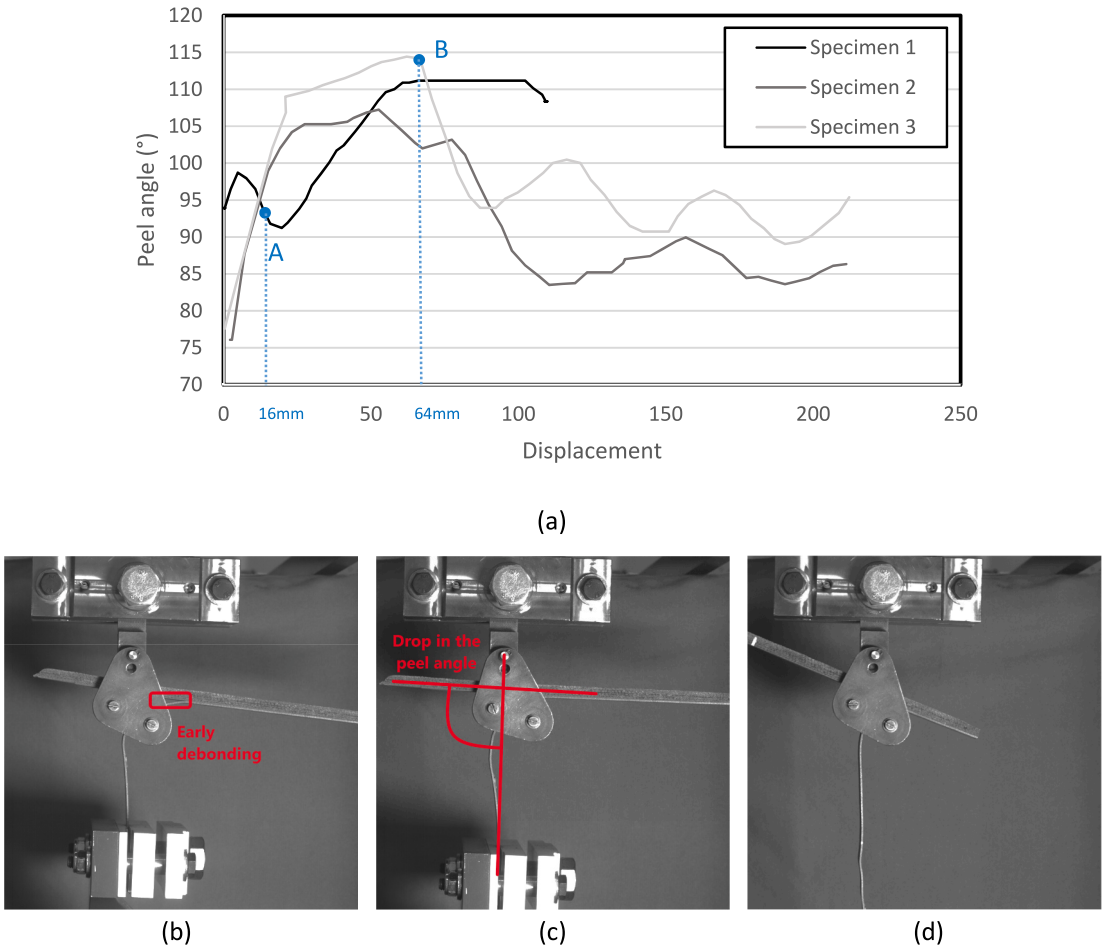

Fig. 10. a) Peel angle-displacement curves for Epoxy Specimens (AxsonSika® ADEKIT A155/H9955), and specimen 1 pictures, b) Zone of early debonding – Image captured at 16 mm of displacement, c) Drop in peel angle – Image captured at 22 mm of displacement, d) Steady peel force – Image captured at 91 mm of displacement.

occur before the steel arm could bend over the roller drum, as shown in Fig. 8.

These findings indicate the unsuitability of the co-curing manufacturing process with epoxy SikaBiresin® CR83 resin, for achieving a strong and reliable adhesion between the carbon steel and FFRP substrates. Further analysis and optimization of the infusion process may be required to improve the resin distribution and enhance the adhesion quality in co-cured joints.

5.2. Epoxy

Fig. 9 shows the load-displacement curves of the peel tests performed in three samples of the Epoxy specimens, and fracture surface for specimen 1. The results show significant scatter between specimens.

Specimen 1 showed a decrease in peel strength between 17 and 41 mm of displacement. Thereafter, the load has increased until reaching a maximum peel load equal to 400 N at 90 mm displacement, where it remained stable for the remaining part of the test.

Specimens 2 and 3 showed different behavior characteristic of stick-slip. In stick-slip behavior, the crack halts at an arrest force and then re-initiates at a higher initiation force in a metastable manner, as Bartlett et al. [46] described.

Fracture analysis of specimen 1 showed 100 % adhesive failure (AF), with all the epoxy remaining on the composite side and no traces of epoxy on the steel surface. The occurrence of adhesive failure is expected as this type of epoxy adhesive is very demanding on substrate surface preparation. However, fracture surface showed a slight color difference between the initial part featuring an area of low adhesion (decrease of peel load – "poor adhesion"), and an area of steady peel force (plateau value of ~400 N). The latest indicates an increase in the adhesion strength at the interface adhesive-steel however not sufficient for the crack to propagate inside the adhesive.

We assume that the poor adhesion observed in the three specimens can be explained by the insufficient surface treatment and cleansing prior to the adhesive application. Dust marks can be observed on the surface, as shown in Fig. 9b).

(b)

Fig. 10 represents the peel angle vs displacement curves of the peel tests performed on the specimens. The peel angle is measured between the plane of the FFRP rigid adherend and the vertical plane which passes through the embedding point of the steel adherend as shown in Fig. 10c).

We notice that peel angle and peel load are related. A decrease in the peel angle results in a drop in the peel load. Points A and B present on both Fig. 9a) and Fig. 10a) show examples of moments of occurrence of drops in both peel angle and peel load for specimen 1 and 3 respectively.

Throughout the tests, the following occurs:

1 Debonding of the flexible adherend from the rigid one prior to the location of the roller (early debonding) – See Fig. 10b).
2 Decrease in the peel load and subsequently peel angle – See Fig. 10c).

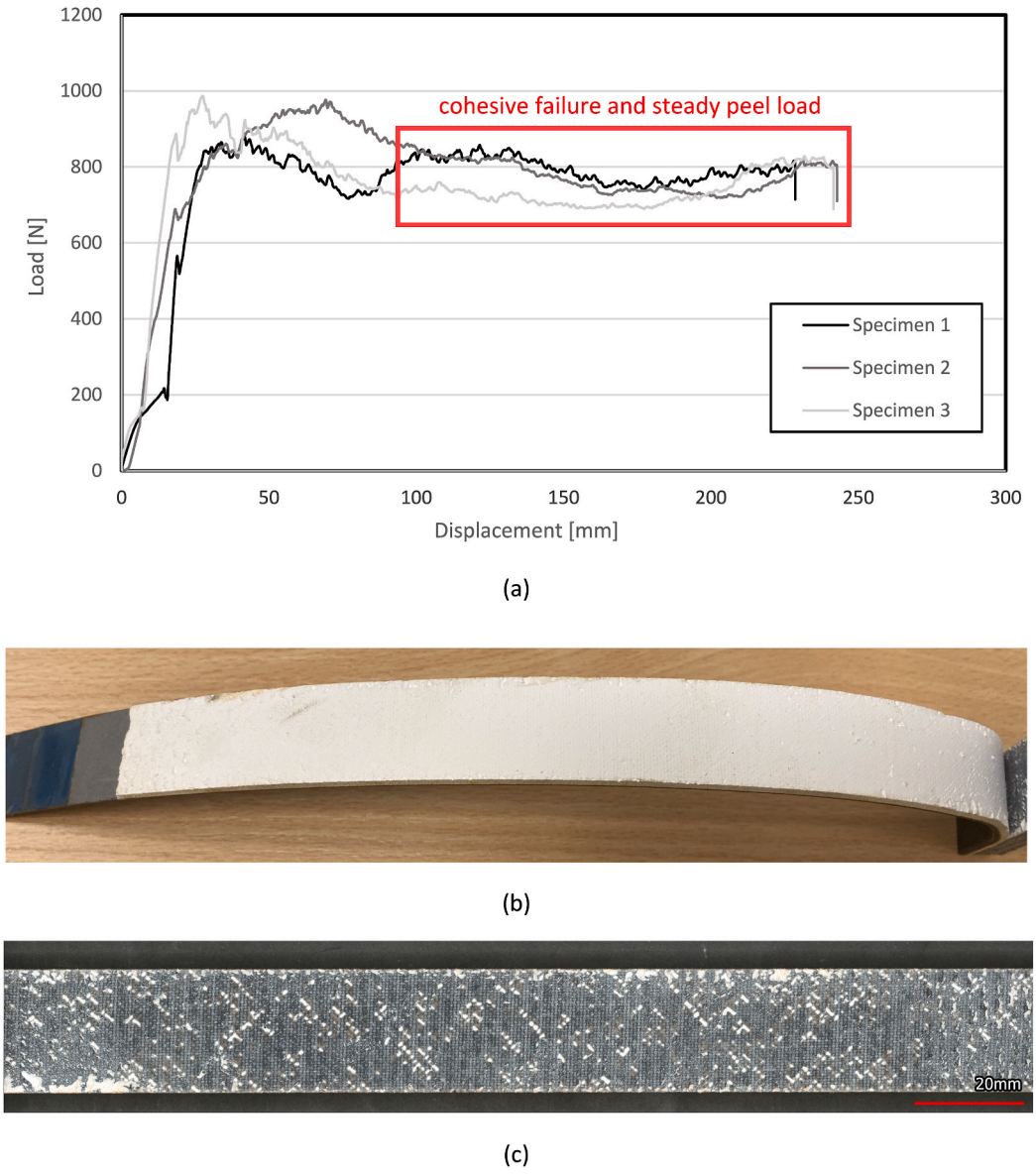

Fig. 11. a) Load-displacement curves for PU specimens (Polyurethane Sikaflex®-554), and corresponding fracture surfaces for specimen 1, a) Steel interface and b) FFRP interface.

This behavior is mainly due to the weak interfacial adhesion of the epoxy adhesive to the steel surface, but the 1.76 mm thick flexible adherend with high flexural stiffness might have also influence the early debonding seen in Fig. 10 a).

These observations suggest that proper surface preparation is crucial for achieving optimal adhesion with the AxsonSika® ADEKIT A155/H9955 epoxy adhesive. Additional investigations and improvements in surface treatment protocols may be necessary to enhance the bonding performance of this adhesive in the tested bonded joints.

5.3. PU

Fig. 11 shows the load-displacement curves of the peel tests performed in three specimens of PU (Polyurethane Sikaflex®-554). All load-displacement curves are consistent and repeatable and the three specimens present similar behaviors with a peel load reaching a plateau value of 800 N approximately.

Fig. 11 also shows the typical fracture surfaces for specimen 1. Notably, 100 % cohesive failure mode was observed, as the PU adhesive is present on both adherends, which clearly indicates good adhesion. This cohesive failure justifies the steady peel load observed in the load-displacement curves. This favorable outcome might be attributed to the improved surface treatment performed prior to the application of the PU adhesive by applying an extra cleansing in the steel surface, the Sika® Aktivator-205 as detailed in subsection 3.1.

Besides, we notice that cohesive failure occurs close to the interface between the FFRP (rigid adherend) and the adhesive. It has been shown in previous studies that due to the asymmetry of the specimens, the failure path is more likely to occur at the interface close to the thin flexible adherend than close to the thick rigid adherend [31, 33]. We assume that the noticed behavior for steel-to-FFRP specimens bonded with PU can be due to the better adhesion between polyurethane and treated carbon steel than between the PU and the FFRP.

Fig. 12 represents the peel angle vs displacement curves of the peel tests performed on the three specimens. The peel angle between the flexible and rigid adherend was constant throughout testing and equal to 114.6° ± 0.7° (average ± standard deviation). This average peel angle was determined over 100 mm of displacement disregarding the first 50 mm, using values of all three specimens. For comparison, in Bartlett's et al. review [46], they reported that floating roller peel test give peel

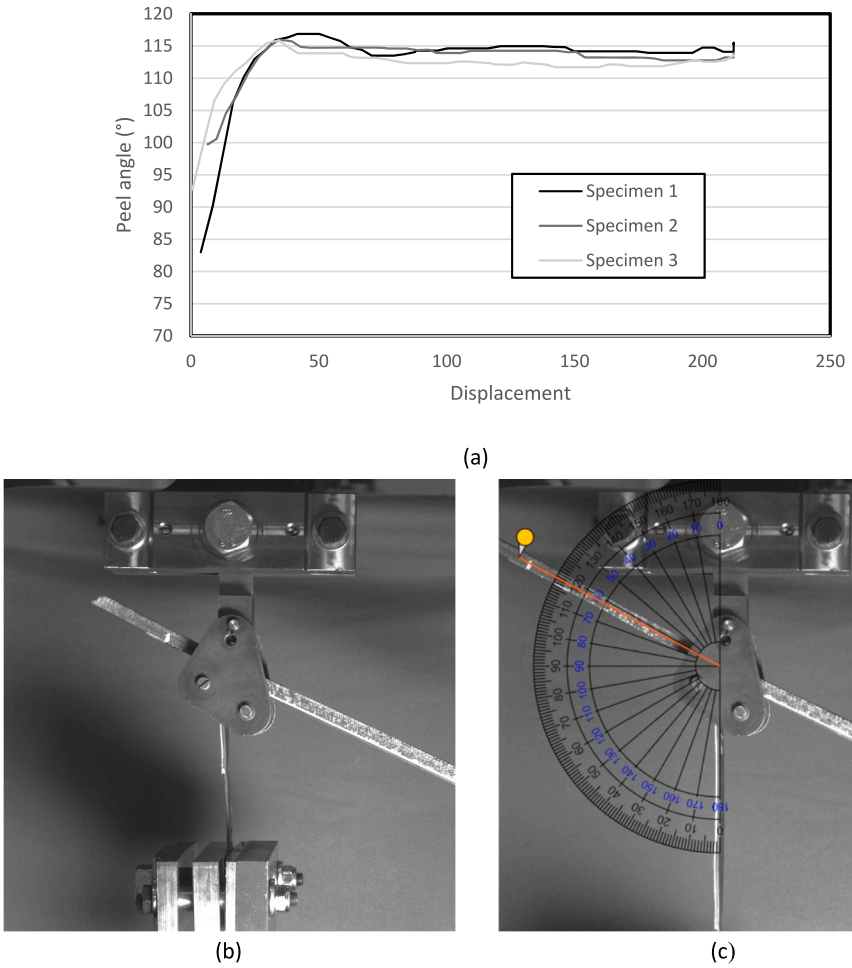

Fig. 12. a) Peel angle-displacement curves for PU specimens (Polyurethane Sikaflex®-554), and specimen 1 pictures, b) Image captured at 76 mm of displacement, c) Image captured at 174 mm of displacement.

angles of nominally 135° when using a roller drum peel test fixture.

These results suggest that the PU adhesive demonstrates promising performance and highlights its potential as a suitable choice for achieving reliable and robust bonding in FFRP-to-steel joints. Furthermore, this finding supports the exploration and development of bio-based PU as an alternative adhesive to synthetic materials. The use of bio-based polyurethane adhesives can contribute to more sustainable and environmentally friendly bonding solutions in various industries.

5.4. BioPU

Fig. 13 shows the load-displacement curves of the peel tests performed in three samples bonded with the BioPU (Castor-oil derived Polyurethane Kehl®), and fractures surfaces of specimen 1, as well as the corresponding measured adhesive thickness through image processing.

Specimen 1 has a peak load at point F_1 (320 N at 18 mm). Thereafter, the peel load decreases significantly to values between 75 and 100 N for displacement ranging between 33 and 135 mm. Finally, it gradually increased reaching 182 N at the end of the test before complete debonding of the flexible adherend. Similar behaviors were observed for Specimen 2 and 3.

The BioPU specimens exhibited challenges related to the control of adhesive thickness. This was shown previously by the adhesive thickness measurement in Table 4 prior to testing and also after testing as it can be observed on fracture surface of the composite rigid adherend in Fig. 13c). BioPU is a bi-component adhesive, which involves reacting an isocyanate with the castor-oil derived polyol. Isocyanate is very sensitive to the room conditions while polymerizing with polyol, as the reaction between isocyanate and water from air humidity produces carbon dioxide that may be trapped in the viscous mixture, which harms the integrity of the adhesive and creates stress concentrators inside the adhesive layer as well as non-adhesive areas in the substrate [47, 48]. Thus, the manufacture process focused on reducing the time exposure time of resin to the environmental conditions. However, by doing so, the viscosity of the resin was not sufficient to prevent leakage in the borders of the plate, which ended up causing some areas with no adhesive between the substrates.

These specimens showed that the thickness of the adhesive layer greatly influenced the peel loads and the mode of failure that occurs on the interface.

Fig. 14a) represents the peel angle vs displacement curves of the peel tests performed on the specimens, and gives a visual representation of the course of testing for specimen 1. During testing of specimen 1, when the adhesive layer thickness was high (before 18 mm of displacement) – See Fig. 14b), the flexible adherend bent smoothly along the curvature of the roller drum. However, as the adhesive thickness reduced, adhesive failure occurred at 18 mm of displacement (Fig. 14c)), resulting in a significant reduction of the peel load and peel angle. Towards the end of the test, between 135 and 182 mm of displacement, the adhesive layer thickness increases, leading to occurrence of cohesive failure in the adhesive, bending of the steel arm, and hence an increase in the peel angle before complete debonding – See Fig. 14d).

These observations highlight the importance of controlling the adhesive layer thickness for achieving consistent and reliable bonding

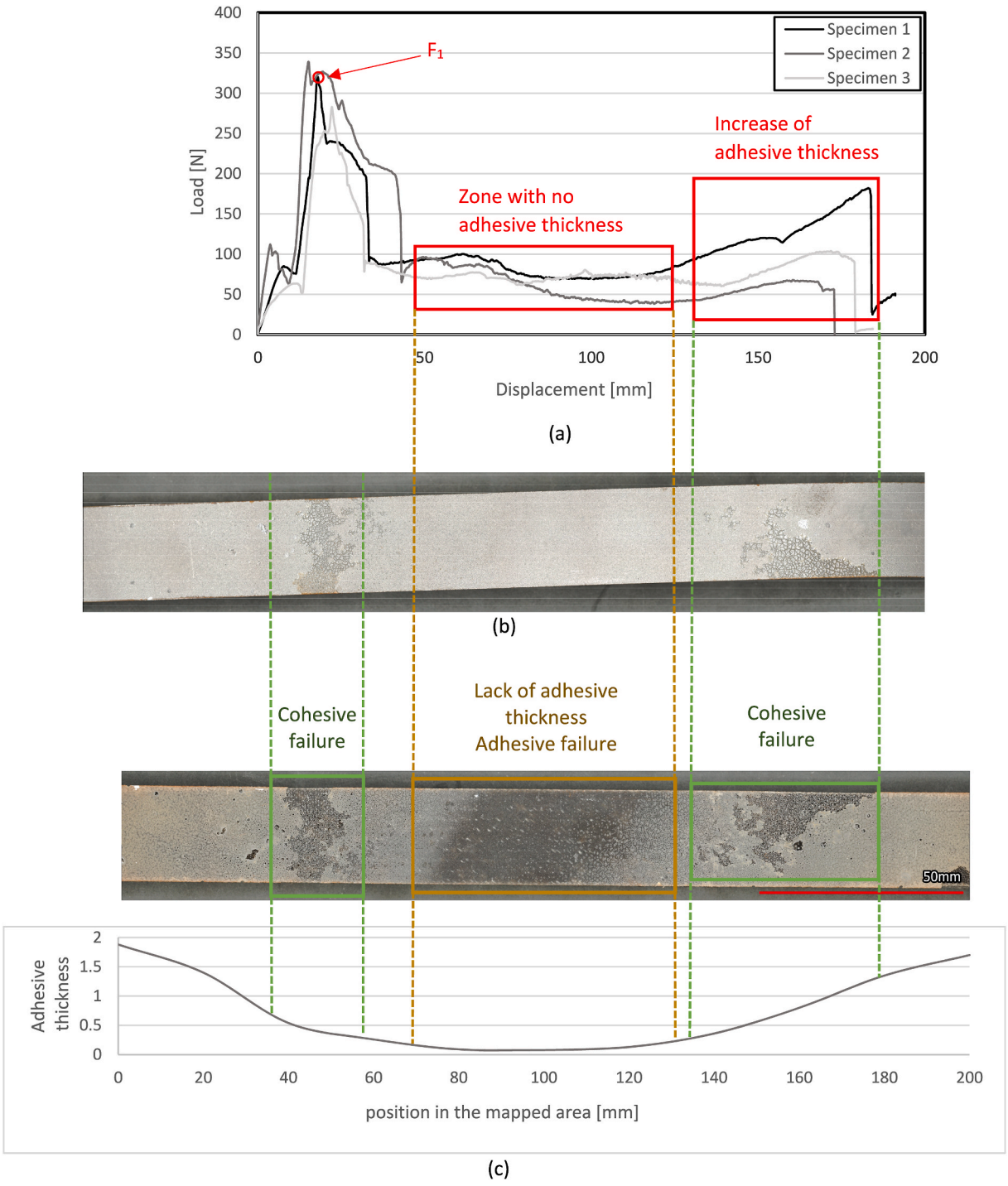

Fig. 13. a) Load-displacement curves for BioPU specimens (Castor-oil derived Polyurethane Kehl®), and fracture surfaces for specimen 1, b) Steel interface and c) FFRP interface and corresponding measured adhesive thickness in the mapped area.

results with the castor-oil derived polyurethane adhesive. Major improvements of the bonding process, and comprehensive understanding of adhesive application, may be necessary to enhance the performance and reliability of this bio-based adhesive, and successfully implement it for structural use.

6. Conclusion

The industrial implementation of sustainable resource derived materials is primary to reduce carbon emissions generated by producing synthetic materials. In this paper, the viability of the use of a newly developed castor-oil derived Polyurethane adhesive was assessed, and compared to the performances of other industrial epoxy and polyurethane adhesives/resins. Floating roller peel tests were performed to evaluate the specimens' interface adhesion. Peel loads, mode of failure and quality of the adhesion for each type of adhesive were evaluated. From the analysis of the obtained results, the following conclusions, and directions of research for future works can be drawn:

- Polyurethane is a promising material for steel-to-FFRP bonded joints. The industrial Polyurethane from Sika® showed high peel loads and full cohesive failure, hence good adhesion. This justifies our interest

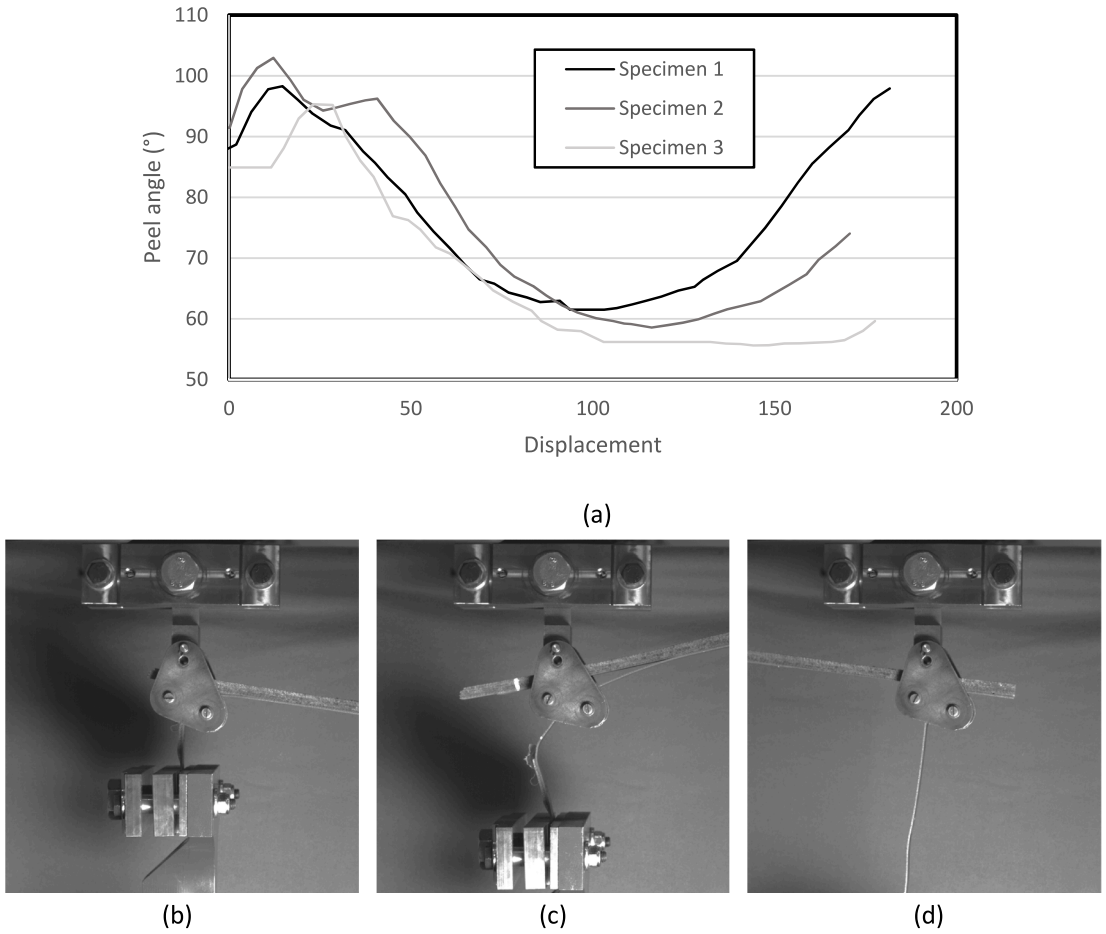

Fig. 14. a) Peel angle-displacement curves for BioPU specimens (Castor-oil derived Polyurethane Kehl®), and specimen 1 pictures, b) Beginning of loading – Image captured at 11 mm of displacement, c) Zone with no adhesive thickness and brutal debonding occurrence – Image captured at 52 mm of displacement, d) Zone with greater adhesive thickness – Image captured at 178 mm of displacement.

towards developing the Kehl® bio-based polyurethane application and industrial implementation.

- The Kehl® castor-oil derived polyurethane showed 14 % cohesive failure on the peeled area. The manufacturing of the joint with this material is very sensitive to moisture exposure and temperature control. Major improvements of the bonding process, including controlling the adhesive application and curing conditions, are necessary to reach higher cohesive failure mode ratio, and thus higher peel loads.
- AxsonSika® ADEKIT A155/H9955 epoxy adhesive unexpectedly showed 100 % adhesive failure and relatively low peel loads. Residual dust on the bonding surface can significantly decrease the adhesion quality, even with high performance adhesives, suggesting the necessity to improve their surface treatments.
- Co-curing bonding technique through the vacuum infusion process displayed low adhesion quality. During the infusion process, insufficient resin flowed at the interface of flax fibers and the steel plate, thus weak adhesion.
- Floating roller peel tests are a quick, easy, and reliable test method to assess the interface adhesion properties for steel-to-composite bonded joints. Peel angles follow the trend with peel loads and could be an alternative measure to assess adhesion.

Declaration of competing interest

There is no conflict of interests.

Data availability

Data will be made available on request.

Acknowledgements

This research was financially supported by CESI LINEACT and COST Action (CA18120) Association under the grant award: E-COST-GRANT-CA18120-e629dae7. The authors would like to acknowledge the support of the GeM Institute of research in Mechanics and Civil Engineering, and the ASM Department of TU Delft (Aeronautics Structures and Materials). This work was supported by FCT, through IDMEC, under LAETA, project UIDB/50022/2020. We would also like to show our sincere appreciation to Sika® for providing the adhesives, and to Sika® Operator Mr. Jean-Pierre Jugé, for his advice and for successfully realizing the bonding of one of the joints used in this study.

References

[1] Mangalgiri PD. Composite materials for aerospace application. Bull Mater Sci 1999; 22:657–64.
[2] Budhe S, Banea MD, de Barros S. Bonded repair of composite structures in aerospace application: a review on environmental issues. Appl Adhes Sci 2018;6 (3).
[3] Taub AI, Krajewski PE, Luo AA, Owens JN. The evolution of technology for materials processing over the last 50 years: the automotive example. JOM 2007;59: 48–57.
[4] de Barros S, Banae MD, Budhe S, de Siqueira CER, Lobão BSP, Souza LFG. Experimental analysis of metal-composite repair of floating offshore units (FPSO). J Adhes 2017;93:147–58.

[5] Zollo RF. Fiber-reinforced concrete: an overview after 30 years of development. Cement Concr Compos 1997;19:107–22.
[6] Van Den Einde L, Zhao L, Seible F. Use of FRP composites in civil structural applications. Construct Build Mater 2003;17:389–403.
[7] Naser MZ, Hawileh RA, Abdalla JA. Fiber-reinforced polymer composites in strengthening reinforced concrete structures: a critical review. Eng Struct 2019; 198.
[8] Katnam KB, Da Silva LFM, Young TM. Bonded repair of composite aircraft structures: a review of scientific challenges and opportunites. Prog Aero Sci 2013; 61:26–42.
[9] Arouche MM, Budhe S, Alves LA, Teixeira de Freitas S, Banez MD, de Barros S. Effect of moisture on the adhesion of CFRP-to-steel bonded joints using peel tests. J Braz Soc Mech Sci Eng 2018;40(10).
[10] Arouche MM, Budhe S, Banea MD, Teixeira de Freitas S, de Barros S. Interlaminar adhesion assessment of carbon-epoxy laminates under salt water ageing using peel tests. Proc Inst Mech Eng Part L 2019;233:1555–63.
[11] Budhe S, Banea MD, de Barros S, da Silva LFM. An update review of adhesively bonded joints in composite materials. Int J Adhesion Adhes 2017;72:30–42.
[12] Rudawska A. Comparaison of the adhesive joints strength of the similar and dissimilar systems of metal alloy/polymer composite. Appl. Adhes. Sci. 2019;7(7).
[13] da Costa Mattos HS, Reis JML, Paim LM, da Silva ML, Lopes Junior R, Perrut VA. Failure analysis of corroded pipelines reinforced with composite repair systems. Eng Fail Anal 2016;59:223–36.
[14] McGeorge D, Echtermeyer AT, Leong KH, Melve B, Robinson M, Fischer KP. Repair of floating offshore units using bonded fibre composite materials. Compos Appl Sci Manuf 2009;40(9):1364–80.
[15] Meniconi LCM, Lana LDM, Morikawa SRK. Experimental fatigue and ageing evaluation of the composite patch repair of a mettalic ship hull. Appl. Adhes. Sci. 2014;2(27).
[16] DNVGL-RP-C301. Design, Fabrication,Operation and qualification of bonded repair of steel structures. 2015.
[17] Li M, Pu Y, Tomas VM, Yoo CG, Ozcan S, Deng Y, Nelson K, Ragauskas AJ. Recent advancements of plant-based natural fiber–reinforced composites and their applications. Compos B Eng 2020;200.
[18] Vigneshwaran S, Sundarakannan R, John KM, Deepark Joel Johnson R, Arun Prasath K, Ajith S, Arumugaprabu V, Uthayakumar M. Recent advancement in the natural fiber polymer composites: a comprehensive review. J Clean Prod 2020;277.
[19] Saheb DN, Jog P. Natural fiber polymer composites: a review. Adv Polym Technol: J. Polym. Proc. Instit. 1999;18(4):351–63.
[20] Baley C. Analysis of the flax fibers tensile behaviour and analysis of the tensile stiffness increase. Compos Appl Sci Manuf 2002;33(7):939–48.
[21] Snoeck D, De Belie N. Mechanical and self-healing properties of cementitious composites reinforced with flax and cottonised flax, and compared with polyvinyl acohol fibers. Biosyst Eng 2012;111(4):325–35.
[22] Baley C, Bourmaud A, Davies P. Eighty years of composites reinforced by flax fibers: a historical review. Compos Appl Sci Manuf 2021;144.
[23] Kim TH, Kweon JH, Choi JH. An experimental study on the effect of overlap length on the failure of composite-to-aluminum single-lap bonded joints. J Reinforc Plast Compos 2008;27(10):1071–81.
[24] Sarlin E, Heinonen E, Vuorinen J, Vippola M, Lepistö T. Adhesion properties of novel corrosion resistant hybrid structures. Int J Adhesion Adhes 2014;49:51–7.
[25] Anyfantis KN, Tsouvalis NG. Loading and fracture response of CFRP-to-steel adhesively bonded joints with thick adherents – Part I: experiments. Compos Struct 2013;96:850–7.
[26] Giampaoli M, Terlizzi V, Rossi M, Chiappini G, Munafo P. Mechanical performances of GFRP-steel specimens bonded with different epoxy adhesives, before and after the aging treatments. Compos Struct 2017;171:145–57.
[27] Lopes J, Stefaniak D, Reis L, Camanho PP. Single lap shear stress in hybrid CFRP/ Steel composites. Procedia Struct Integr 2016;1:58–65.
[28] Tamakrishnan KR, Sarlin E, Kanerva M, Hokka M. Experimental study of adhesively bonded natural fiber composite - steel hybrid laminates. Composites Part C: Open Access 2021;5.
[29] Hart-Smith LJ. A peel-type durability test coupon to assess interfaces in bonded, co-bonded, and co-cured composite sructures. Int J Adhesion Adhes 1999;19(2–3): 181–91.
[30] Sargent JP. Durability studies for aerospace applications using peel and wedge tests. Int J Adhesion Adhes 2005;25(3):247–56.
[31] Teixeira de Freitas S, Sinke J. Method to assess interface adhesion in composite bonding. Appl. Adhes. Sci. 2015;3(9).
[32] Teixeira de Freitas S, Sinke J. Adhesion properties of composite-to-aluminium joints using peel tests. J Adhes 2013;90(5–6):511–25.
[33] Teixeira de Freitas S, Banea M, Budhe S, de Barros S. Interface adhesion assessment of composite-to-metal bonded joints under salt spray conditions using peel tests. Compos Struct 2017;164:68–75.
[34] Pereira JPO, Campilho RGSG, Novoa PJRO, Silva FJG, Gonçalves DC. Adherend effect on the peel strength of a brittle adhesive. Procedia Struct Integr 2022;37: 722–9.
[35] Gnädinger F, Middendorf P, Fox B. Interfacial shear strength studies of experimental carbon fibres, novel thermosetting polyurethane and epoxy matrices and bespoke sizing agents. Compos Sci Technol 2016;133:104–10.
[36] Galvez P, de Armentia SL, Abenojar J, Martinez MA. Effect of moisture and temperature on thermal and mechanical properties of structural polyurethane adhesive joints. Compos Struct 2020;247.
[37] Weiss J, Voigt M, Kunze C, Huacuja Sànchez JE, Possart W, Grundmeier G. Ageing mechanisms of polyurethane adhesive/steel interfaces. Int J Adhesion Adhes 2016; 70:167–75.
[38] Sika®. SikaBiresin® CR83 data sheet [Online]. Available: https://fra.sika.com/content/dam/dms/fr01/z/fr-np-ind-sikabiresin-cr83-fr.pdf.
[39] Sika®. ADEKIT A155/H9955 Data sheet [Online]. Available: https://fra.sika.com/content/dam/dms/fr01/t/fr-np-ind-adekit-a155-h9955.pdf.
[40] Sika®. Sikaflex®-554 data sheet [Online]. Available: https://industry.sika.com/content/dam/dms/fr01/k/sikaflex-554.pdf.
[41] de Mouara AP, da Silva EHP, dos Santos VS, Galera MF, Sales FCP, Elizario S, de Moura MR, Rigo VA, da Costa RRC. Structural and mechanical characterization of polyurethane-CaCO3 composites synthesized at high calcium carbonate loading: an experimental and theoretical study. J Compos Mater 2021;55(21).
[42] Sika®. Sika® aktivator-205 data sheet [Online]. Available: https://che.sika.com/content/dam/dms/ch01/u/sika-aktivator-205.pdf.
[43] standard The ISO 4287 1997. Geometrical Product Specifications (GPS). Surface texture: Profile method. Terms, definitions and surface texture parameters. 1997.
[44] Ghumatkar A, Sekhar R, Budhe S. Experimental study on different adherend surface roughness on the adhesive bond strength. Mater Today Proc 2017;4(8): 7801–9. 4.
[45] ASTM D3167. Standard test method for floating roller peel resistance of adhesive. 2010.
[46] Bartlett MD, Case SW, Kinloch AJ, Dillard DA. Peel tests for quantifying adhesion and toughness: a review. Prog Mater Sci 2023;137.
[47] Wan YZ, Hong L, Jia SR, Huang Y, Zhu Y, Wang L, Jiang HJ. Synthesis and characterization of hydroxyapatite-bacterial cellulose nanocomposites. Compos Sci Technol 2006;66(11–12):1825–32.
[48] Silva EHP, Aguiar JCF, Waldow G, Costa RRC, Tita V, Ribeiro ML. Compression and morphological properties of a bio-based polyurethane foam with Aluminum hydroxide. Proceedings of the Institute of Mechanical Engineers, Part L: Journal of Materials: Design and Applications 2022;236(7):1408–18.